

Electronic Supplementary Information for:

Heteroaromatic ring modified naphthalimide interlayer materials for efficient polymer solar cells[†]

Shuixing Dai,^{a,#,*} Jilei Jiang,^{a,#} Liangmin Yu,^b Lunxiu Cui,^a Xu Zhang,^c Canhui Zhang,^a

Ke Gao,^c Heqing Jiang^d and Minghua Huang^{a,*}

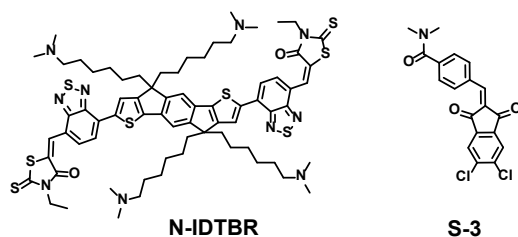
^a School of Materials Science and Engineering, Ocean University of China, Qingdao 266100, China. E-mail: daishuixing@ouc.edu.cn

^b Key Laboratory of Marine Chemistry Theory and Technology of Ministry of Education, Ocean University of China, Qingdao 266100, China

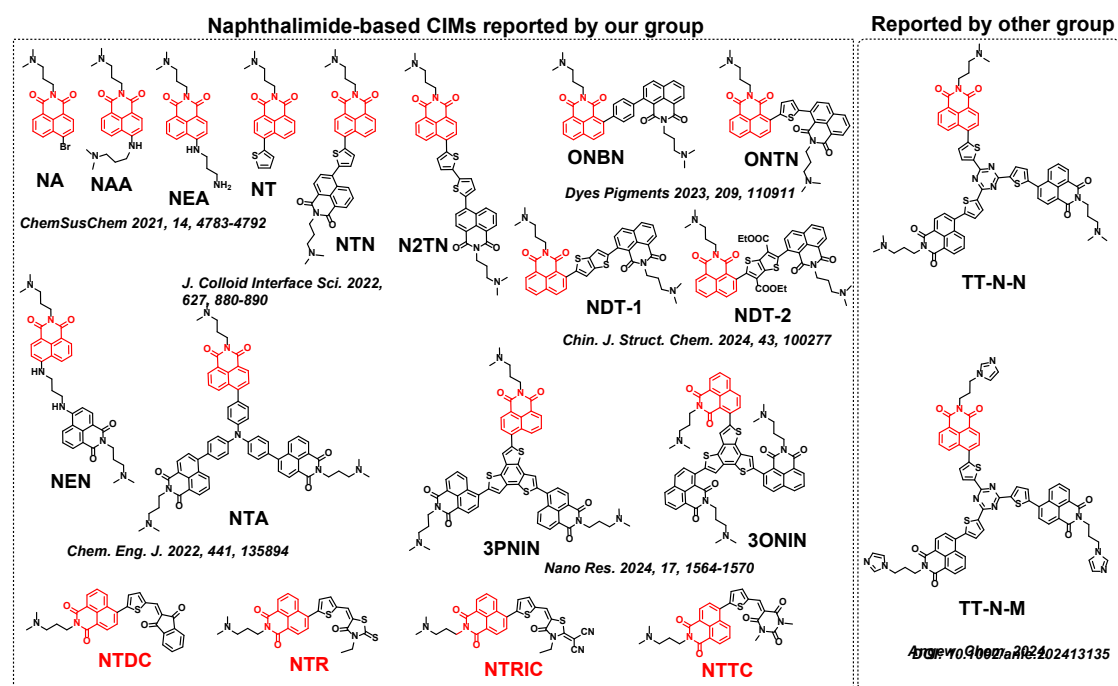
^c School of Chemistry and Chemical Engineering, Shandong University, Qingdao, 266237, China

^d Key Laboratory of Photoelectric Conversion and Utilization of Solar Energy, Qingdao Institute of Bioenergy and Bioprocess Technology, Chinese Academy of Sciences, Qingdao, 266101, China

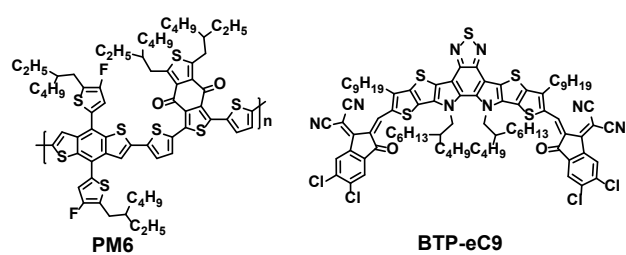
(a)



(b)



(c)



(d)

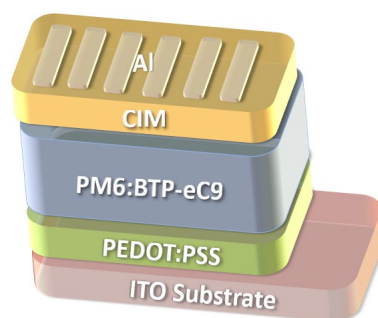


Fig. S1 The molecular structures of (a) N-IDTBR ¹, S-3 ², (b) NI-based CIMs, (c) PAL materials (PM6 ³, and BTP-eC9 ⁴), and (d) PSC device structure used in this study.

Materials

The chemical reagents and solvents used were obtained commercially. PM6 and BTP-eC9 used in this study were supplied by Derthon Optoelectronic Materials Science Technology Co., Ltd. and Solarmer Materials Inc., respectively. PEDOT: PSS (Clevios™ PVP Al 4083) was purchased from J&K Scientific.

Methods

¹H-NMR and ¹³C-NMR were probed by a Bruker Advance III 600 MHz instrument with tetramethyl silane as the internal reference. ESI-MS mass spectrometry data was obtained on Thermo-QE plus. TGA measurements were carried out using a thermogravimetric analyzer (Netzsch TG 209 F3) under flowing nitrogen gas at a heating rate of 10 °C/min. UV-vis absorption spectra were performed on Shimadzu UV-vis 2910 spectrophotometer in chloroform solution and thin film (on a quartz substrate). Electrochemical measurements were carried out in anhydrous acetonitrile with tetra-n-butylammonium hexafluorophosphate (0.1 M) as a supporting electrolyte at a scan rate of 50 mV/s employing a computer-controlled CHI660E electrochemical workstation in three-electrode electrochemical cell (Pt wire as counter electrode, glassy carbon electrode as working electrode, and saturated Hg/HgCl electrode as reference electrode). The potentials were referenced to a ferrocenium/ferrocene (FeCp₂⁺⁰) couple using ferrocene as an external standard. Electron paramagnetic resonance (EPR) was measured by EMXplus-6/1 (Bruker). The surface morphologies of the films were observed employing a AFM 5500 (Agilent) in the tapping mode. Film thickness of organic layer was measured by Dektak XT (Bruker).

XRD characterization. The XRD patterns were obtained by Bruker D8 Advance (Cu K α radiation). The samples are prepared on silicon substrate by spin coating. The stacking distance is calculated by Bragg's law. The calculation formula is as follows:

$$d = \frac{n\lambda}{2\sin\theta}$$

Where n equal to 1, and λ is 0.15406 nm.

Fabrication and characterization of PSCs. The devices were fabricated with the structure of ITO/PEDOT: PSS/PM6: BTP-eC9 blend/CIM/Al in the glove box. The ITO glass (sheet resistance = $15 \Omega \text{ sq}^{-1}$) was precleaned in an ultrasonic bath with deionized water, acetone, and isopropanol subsequently, and treated in an UV/ozone for 5 min. PEDOT:PSS was spin-coated on ITO glass at 4000 rpm for 30 s and then annealed at $150 \text{ }^\circ\text{C}$ for 15 min in air. The blend of PM6: BTP-eC9 (1:1.2, w/w, 17 mg mL^{-1} in total), which was dissolved in chloroform with 0.5% DIO (v/v), or PM6: PC₆₁BM (1:1.5, w/w, 18 mg mL^{-1} in total in chloroform) was spin-coated on PEDOT: PSS layer (*ca.* 100 nm). Then the CIMs (NTDC, NTR, NTRIC, NTTC, NTN, and PDINO), which were dissolved in methanol with the concentration of 1 mg mL^{-1} , were spin-coated on the PM6: BTP-eC9 active layer with a thickness of 10 nm. Finally, Al was evaporated as cathode electrode (*ca.* 80 nm) under $4 \times 10^{-4} \text{ Pa}$. The active area of each device was 0.05 cm^2 . The J - V curve was measured using a computer-controlled Keithley 2400 workstation along with simulated AM 1.5G spectra (100 mW cm^{-2}). A $2 \times 2 \text{ cm}^2$ monocrystalline silicon reference cell (SRC-1000-TC-QZ) was purchased from VLSI Standards Inc. The EQE spectrum was measured using a solar cell spectral response measurement system QE-R3011 (Enli Technology Ltd., Taiwan). The light intensity at each wavelength was calibrated using a standard single crystal Si photovoltaic cell.

Mobility Measurements. The electron-only devices of CIM neat film were fabricated using the structure of ITO/CIMs/Ag. The details are as follows: the pre-cleaned ITO glass was spin-coated with CIMs (*ca.* 60 nm), then Ag (*ca.* 80 nm) was evaporated under vacuum ($4 \times 10^{-4} \text{ Pa}$).

Hole- or electron-only devices were fabricated using the structure of ITO/PEDOT: PSS/ PM6: BTP-eC9/Au for holes and ITO/ZnO/PM6: BTP-eC9/CIM/Ag for electrons. For hole-only devices, the pre-cleaned ITO glass was spin-coated with PEDOT: PSS, PM6: BTP-eC9 blend was spin-coated same as photovoltaic devices, then Au (*ca.* 80 nm) was evaporated under vacuum ($4 \times 10^{-4} \text{ Pa}$). For electron-only devices, the pre-cleaned ITO glass was spin-coated with ZnO (ZnO layer was prepared with ZnO precursor solution (a mixture of zinc acetate dehydrate (100 mg), 2-methoxyethanol

(973 μL) and ethanolamine (28.29 μL) stirred overnight) at 4000 rpm, and then baked at 200 $^{\circ}\text{C}$ for 30 min), then PM6: BTP-eC9 blend and CIMs were spin-coated subsequently, then Ag (*ca.* 80 nm) was evaporated under vacuum. The mobility was extracted by fitting the current density–voltage curves via the SCLC method.⁵ The calculation formula is as follows:

$$J = \frac{9\varepsilon_0\varepsilon_r\mu V^2}{8d^3}$$

Where J represents the current density, ε_r and ε_0 are the relative dielectric and vacuum dielectric constant, respectively, V is the voltage drop, and d is *ca.* 80 nm.

EIS test. EIS test was conducted on the CHI660E electrochemical workstation in two-electrode system. The device preparation for EIS test is consistent with J - V characterization. The working electrode is connected to ITO (as positive electrode), and the counter electrode and reference electrode are connected to Ag electrode (as negative electrode) at the same time, and a bias voltage equal to V_{OC} was applied to dissipate the total current.

Conductivity measurements. The films of CIMs were spin-coated on substrates at a film thickness (T) of *ca.* 50 nm. The parallel aluminum electrodes (*ca.* 80 nm) at length (L) of 12 mm were evaporated on CIMs. The separation distance (D) between the two parallel electrodes was 1 mm. Conductivity measurements were carried out using a Keithley 2400 workstation. The calculation formula is as follows:

$$\sigma = ID/VLT$$

Synthesis of NTDC, NTR, NTRIC, and NTTC.

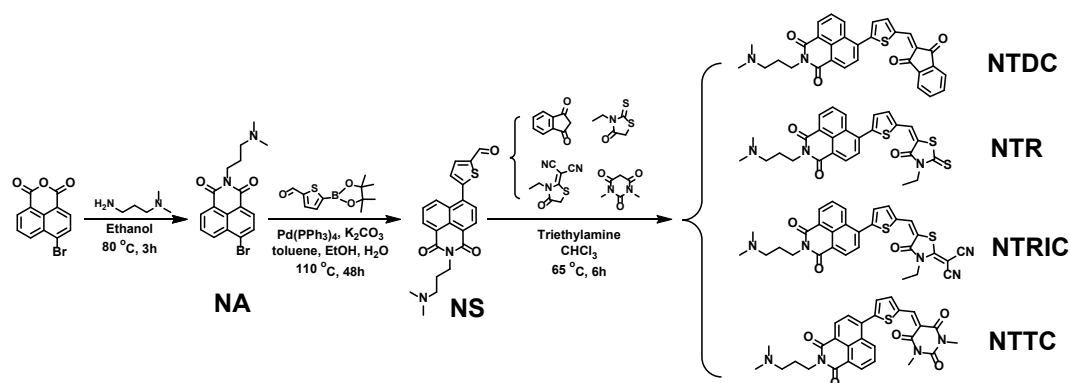


Fig. S2 Synthesis routes of NTDC, NTR, NTRIC, and NTTC.

Synthesis of NS: The NA intermediate was synthesized according to previously reported method.⁶ NA (500 mg, 1.38 mmol), 5-(4,4,5,5-tetramethyl-1,3,2-dioxaborolan-2-yl) thiophene-2-carbaldehyde (395.49 mg, 1.66 mmol), toluene (15 mL) EtOH (5 mL) and saturated K₂CO₃ solution (2 mL) were mixed in a two-neck round-bottomed flask. Then Pd(PPh₃)₄ (45 mg, 0.039 mmol) was added after the degasification with dry nitrogen. Then the mixture was stirred at 110 °C for 48 hours under a nitrogen atmosphere. After the mixture was cooled to room temperature, the crude product was purified by extraction and silica gel column chromatography with methanol/chloroform (1:3, v/v) as eluent. The yellow solid NS was obtained with a yield of 70%. ¹H NMR (600 MHz, CDCl₃) δ 10.00 (s, 1H), 8.65 (d, *J* = 7.2 Hz, 1H), 8.62 (d, *J* = 7.5 Hz, 1H), 8.51 (d, *J* = 8.5 Hz, 1H), 7.89 (d, *J* = 3.8 Hz, 1H), 7.84 (d, *J* = 7.5 Hz, 1H), 7.79 (t, *J* = 7.9 Hz, 1H), 7.43 (d, *J* = 3.8 Hz, 1H), 4.25 (t, *J* = 7.5 Hz, 2H), 2.52 (t, *J* = 7.4 Hz, 2H), 2.31 (s, 6H), 1.99-1.95 (m, 2H). ¹³C NMR (151 MHz, CDCl₃) δ 181.86, 162.94, 162.66, 148.21, 143.99, 136.40, 135.46, 130.68, 130.58, 129.51, 128.73, 128.63, 127.89, 127.67, 126.78, 122.13, 122.00, 55.93, 43.98, 37.72, 28.68.

Synthesis of NTDC: A mixture of NS (300 mg, 0.76 mmol), 1,3-indanedione (134.05 mg, 0.92 mmol), CHCl₃ (15 mL) and triethylamine (1 mL) in a two-neck round bottomed flask was stirred at 65 °C for 6 hours. After the mixture was cooled to room temperature and removed the solvent, the crude product was purified by silica gel

column chromatography with methanol/chloroform (1:5, v/v) as eluent. The yellow-green solid **NTDC** was obtained with a yield of 75%. ^1H NMR (600 MHz, CDCl_3) δ 8.68 (d, $J = 8.4$ Hz, 1H), 8.65 (d, $J = 7.5$ Hz, 1H), 8.62 (d, $J = 8.5$ Hz, 1H), 8.10 (d, $J = 4.0$ Hz, 1H), 8.05 (s, 1H), 8.03-7.99 (m, 2H), 7.95 (d, $J = 7.6$ Hz, 1H), 7.83 (s, 1H), 7.82 (d, $J = 5.5$ Hz, 2H), 7.49 (d, $J = 3.9$ Hz, 1H), 4.28 (t, $J = 7.5$ Hz, 2H), 2.59 (t, $J = 7.3$ Hz, 2H), 2.38 (s, 6H), 2.05-2.01 (m, 2H). ^{13}C NMR (151 MHz, CDCl_3) δ 189.99, 189.62, 164.04, 163.78, 151.85, 142.19, 142.10, 140.58, 139.01, 137.78, 135.46, 135.41, 135.26, 131.89, 131.67, 130.58, 130.09, 129.67, 128.98, 128.82, 127.79, 125.59, 123.31, 123.15, 123.05, 122.97, 57.05, 44.99, 38.74, 25.63. ESI-MS (m/z): $[\text{M} + \text{H}]^+$ calculated for $\text{C}_{31}\text{H}_{24}\text{N}_2\text{O}_4\text{S}$: 521.60, found: 521.15.

Synthesis of NTR: A mixture of **NS** (260 mg, 0.66 mmol), 3-ethylrhodanine (128.18 mg, 0.80 mmol), CHCl_3 (15 mL), triethylamine (2 mL) in a two-neck round bottomed flask was stirred at 65 °C for 6 hours. After removing the solvent, the crude product was purified by silica gel column chromatography with methanol/chloroform (1:3, v/v) as eluent. The dark orange solid **NTR** was obtained with a yield of 72%. ^1H NMR (600 MHz, CDCl_3) δ 8.67 (d, $J = 7.2$ Hz, 1H), 8.63 (d, $J = 7.5$ Hz, 1H), 8.59 (d, $J = 8.3$ Hz, 1H), 7.93 (s, 1H), 7.88 (d, $J = 7.5$ Hz, 1H), 7.82 (t, $J = 7.9$ Hz, 1H), 7.54 (d, $J = 3.9$ Hz, 1H), 7.44 (d, $J = 3.9$ Hz, 1H), 4.29 (t, $J = 7.2$ Hz, 2H), 4.21 (q, $J = 7.2$ Hz, 2H), 2.77 (t, $J = 7.5$ Hz, 2H), 2.52 (s, 6H), 2.13-2.09 (m, 2H), 1.31 (t, $J = 7.2$ Hz, 3H). ^{13}C NMR (151 MHz, CDCl_3) δ 191.70, 167.28, 163.99, 163.71, 147.03, 139.92, 137.39, 134.25, 131.66, 131.63, 130.57, 130.44, 129.58, 128.86, 128.76, 127.76, 124.34, 123.15, 122.93, 122.57, 57.17, 45.23, 40.06, 38.88, 25.90, 12.30. ESI-MS (m/z): $[\text{M} + \text{H}]^+$ calculated for $\text{C}_{27}\text{H}_{25}\text{N}_3\text{O}_3\text{S}_3$: 536.70, found: 536.11.

Synthesis of NTRIC: A mixture of **NS** (240 mg, 0.61 mmol), 2-(3-ethyl-4-oxothiazolidin-2-ylidene)malononitrile (141.79 mg, 0.73 mmol), CHCl_3 (15 mL), triethylamine (1.5 mL) in a two-neck round bottomed flask was stirred at 65 °C for 6 hours. Then the mixture was cooled to room temperature and removed the solvent, the crude product was purified by silica gel column chromatography with methanol/dichloromethane (1:5, v/v) as eluent. The red solid **NTRIC** was obtained with

a yield of 69%. ^1H NMR (600 MHz, CDCl_3) δ 8.68 (d, $J = 7.4$ Hz, 1H), 8.64 (d, $J = 7.5$ Hz, 1H), 8.55 (d, $J = 8.4$ Hz, 1H), 8.15 (s, 1H), 7.90 (d, $J = 7.5$ Hz, 1H), 7.84 (t, $J = 7.9$ Hz, 1H), 7.62 (d, $J = 4.1$ Hz, 1H), 7.49 (d, $J = 4.1$ Hz, 1H), 4.35 (q, $J = 7.2$ Hz, 2H), 4.29 (t, $J = 7.2$ Hz, 2H), 2.81 (t, $J = 7.7$ Hz, 2H), 2.54 (s, 6H), 2.15-2.10 (m, 2H), 1.43 (t, $J = 7.2$ Hz, 3H). ^{13}C NMR (151 MHz, CDCl_3) δ 165.78, 165.12, 163.97, 163.69, 147.93, 138.66, 137.03, 135.39, 131.87, 131.64, 130.80, 130.68, 129.55, 129.05, 128.85, 128.05, 127.99, 123.00, 115.82, 112.92, 111.91, 56.57, 44.24, 40.86, 38.33, 29.71, 24.84, 14.22. ESI-MS (m/z): $[\text{M} + \text{H}]^+$ calculated for $\text{C}_{30}\text{H}_{25}\text{N}_5\text{O}_3\text{S}_2$: 568.68, found: 568.15.

Synthesis of NTTC: A mixture of NS (200 mg, 0.51 mmol), 1,3-dimethylbarbituric acid (95.48 mg, 0.61 mmol), CHCl_3 (15 mL), triethylamine (1 mL) in a two-neck round bottomed flask was stirred at 65 °C for 6 hours. After removing the solvent, the crude product was purified by silica gel column chromatography with methanol/chloroform (1:5, v/v) as eluent. The orange solid NTTC was obtained with a yield of 77%. ^1H NMR (600 MHz, CDCl_3) δ 8.77 (s, 1H), 8.67 (d, $J = 7.3$ Hz, 1H), 8.63 (d, $J = 7.5$ Hz, 1H), 8.58 (d, $J = 8.5$ Hz, 1H), 8.00 (d, $J = 4.0$ Hz, 1H), 7.95 (d, $J = 7.6$ Hz, 1H), 7.85-7.81 (m, 1H), 7.53 (d, $J = 3.9$ Hz, 1H), 4.33 (t, $J = 6.9$ Hz, 2H), 3.45 (d, $J = 11.5$ Hz, 6H), 3.13 (t, $J = 7.9$ Hz, 2H), 2.80 (s, 6H), 2.30 (t, $J = 7.9$ Hz, 2H). ^{13}C NMR (151 MHz, CDCl_3) δ 164.07, 163.82, 162.44, 161.98, 155.01, 151.20, 148.32, 145.47, 138.41, 138.06, 132.22, 131.97, 130.78, 129.82, 129.67, 129.10, 128.79, 127.93, 122.71, 122.66, 111.32, 56.22, 43.47, 37.71, 29.06, 28.26. ESI-MS (m/z): $[\text{M} + \text{H}]^+$ calculated for $\text{C}_{28}\text{H}_{26}\text{N}_4\text{O}_5\text{S}$: 531.60, found: 531.17.

NMR spectra of NS, NTDC, NTR, NTRIC, and NTTC.

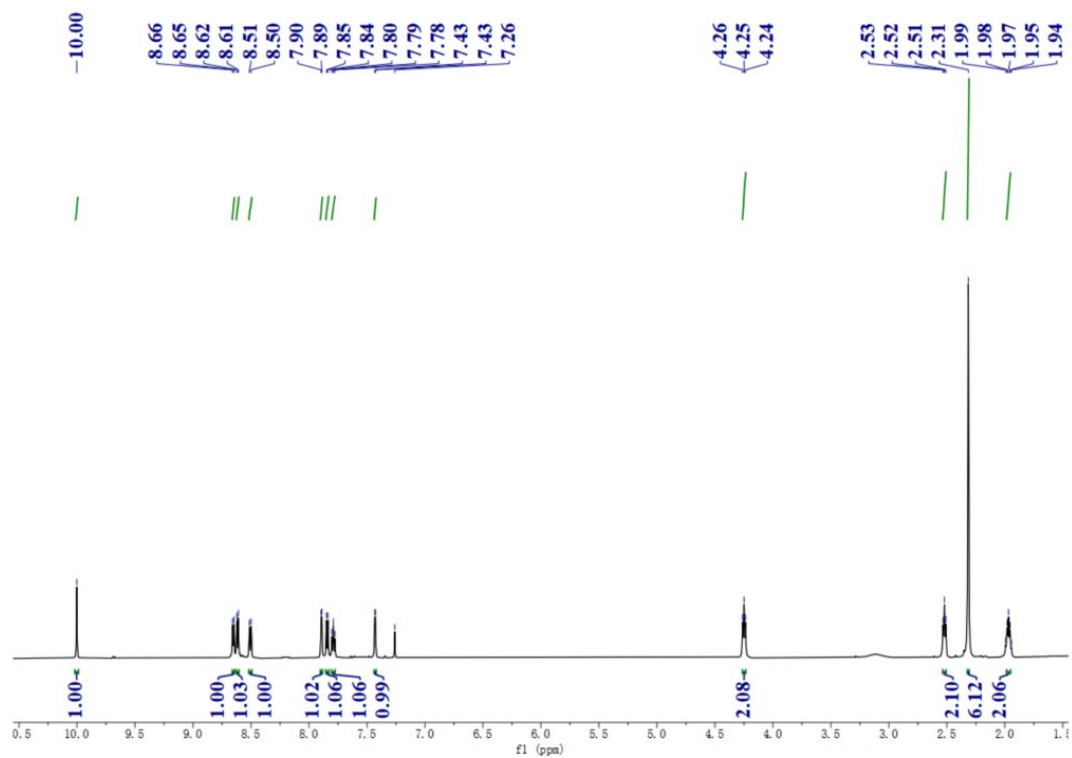


Fig. S3 ¹H NMR spectrum of NS.

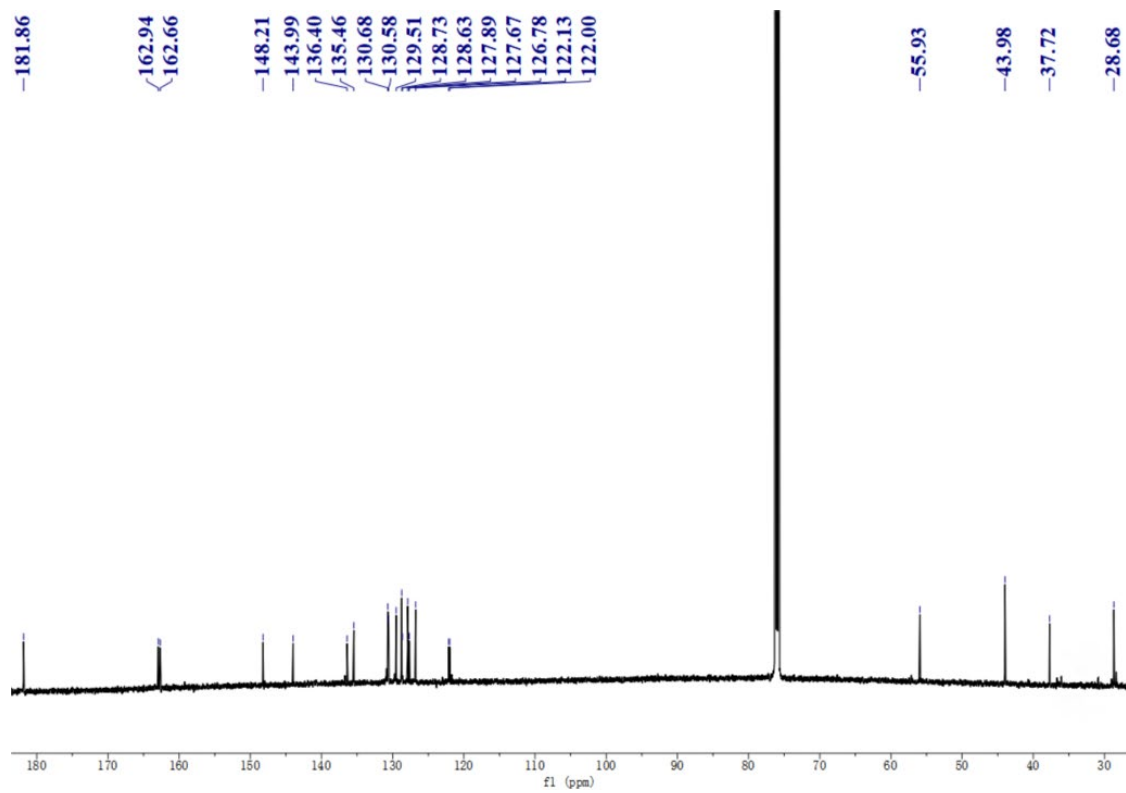


Fig. S4 ¹³C NMR spectrum of NS.

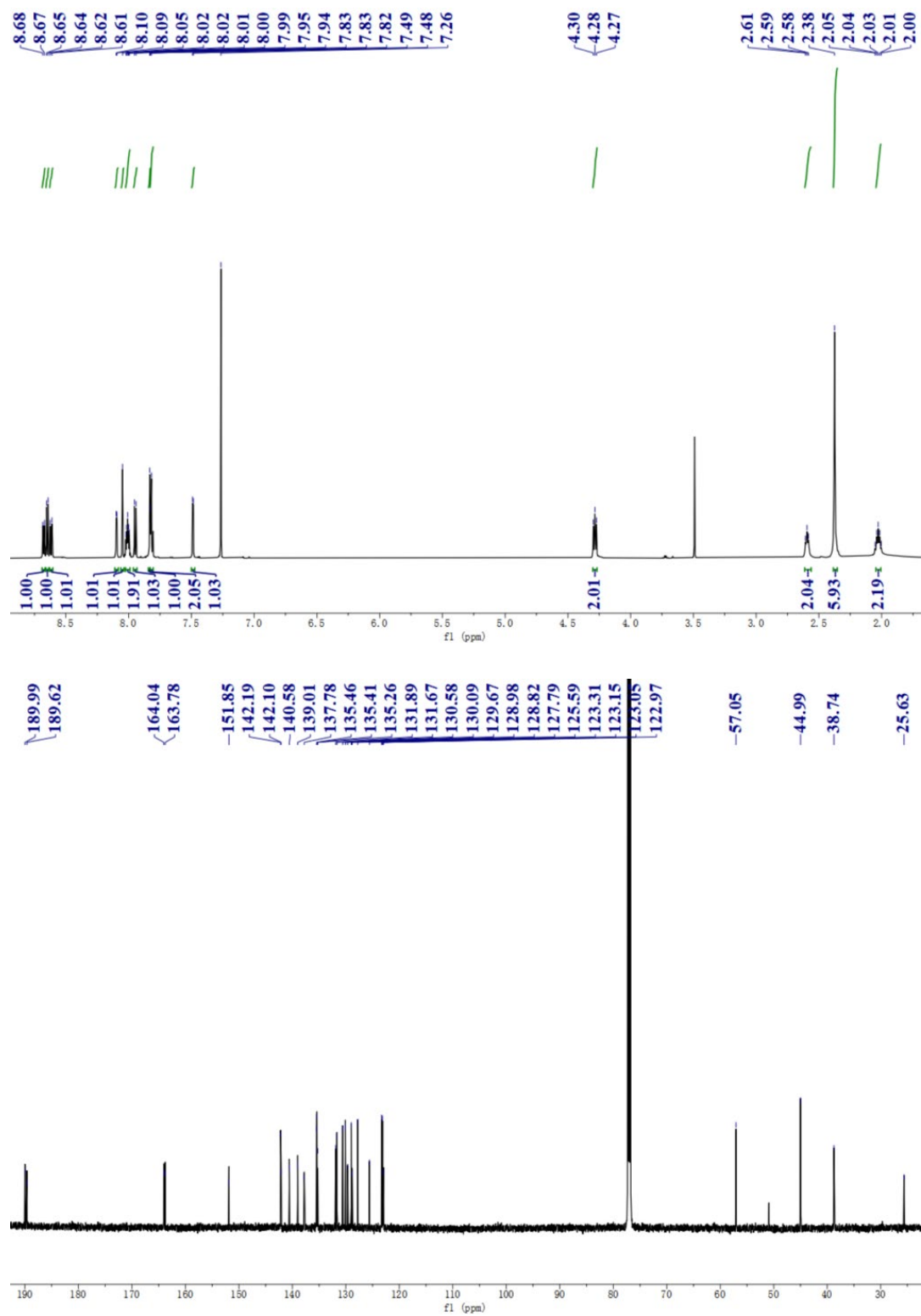


Fig. S5 ^1H NMR (top) and ^{13}C NMR (bottom) spectra of NTDC.

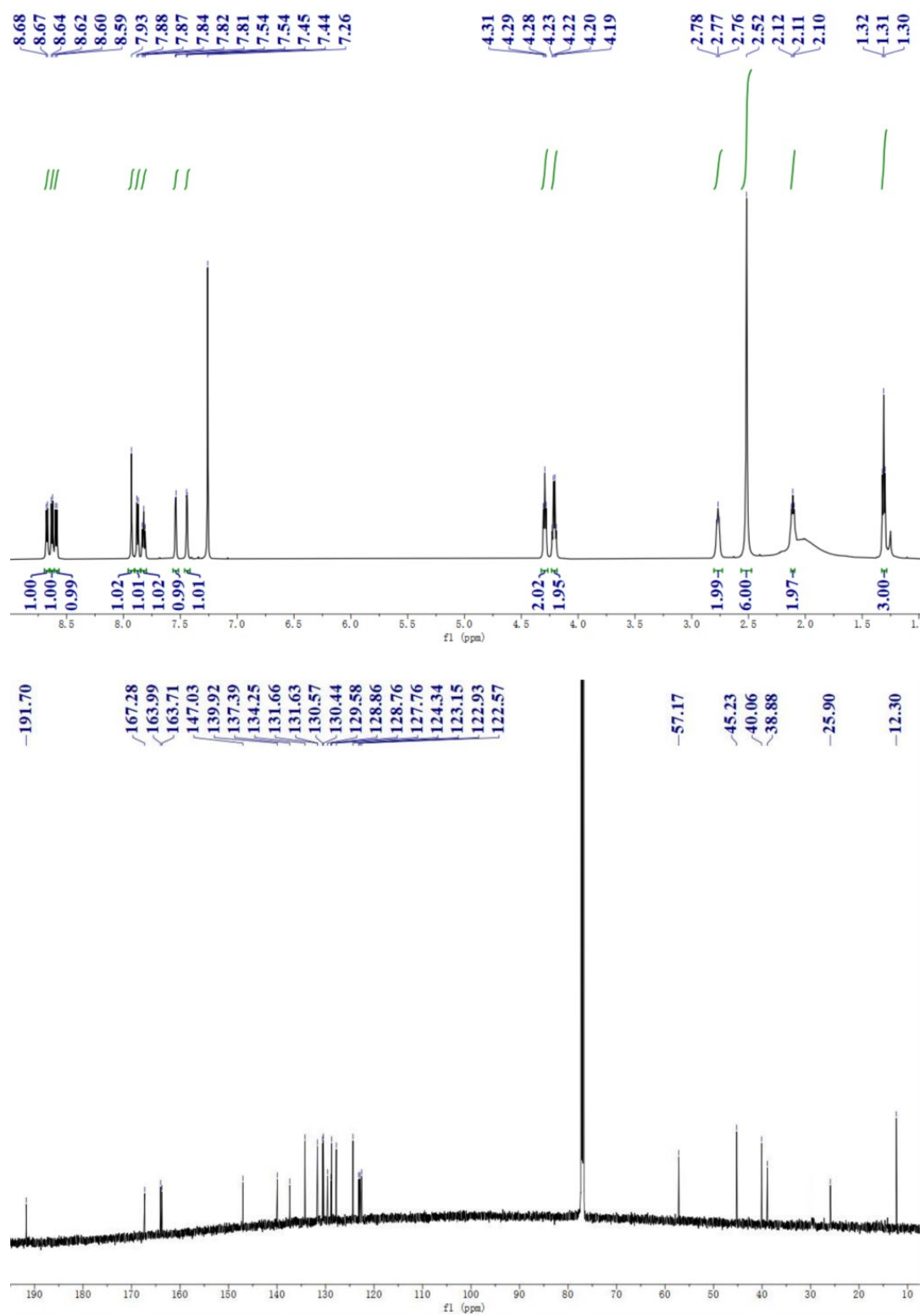


Fig. S6 ^1H NMR (top) and ^{13}C NMR (bottom) spectra of NTR.

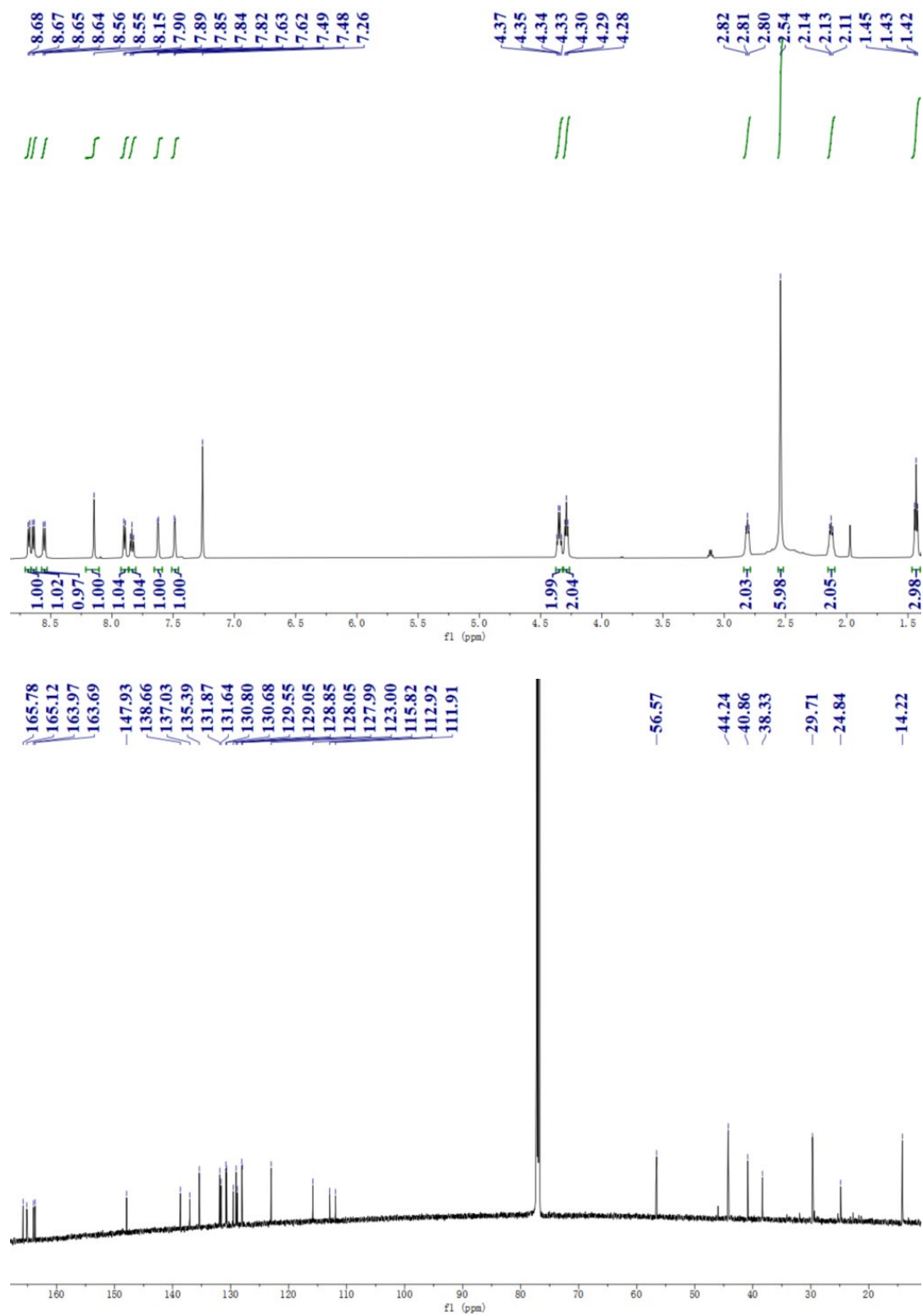


Fig. S7 ^1H NMR (top) and ^{13}C NMR (bottom) spectra of NTRIC.

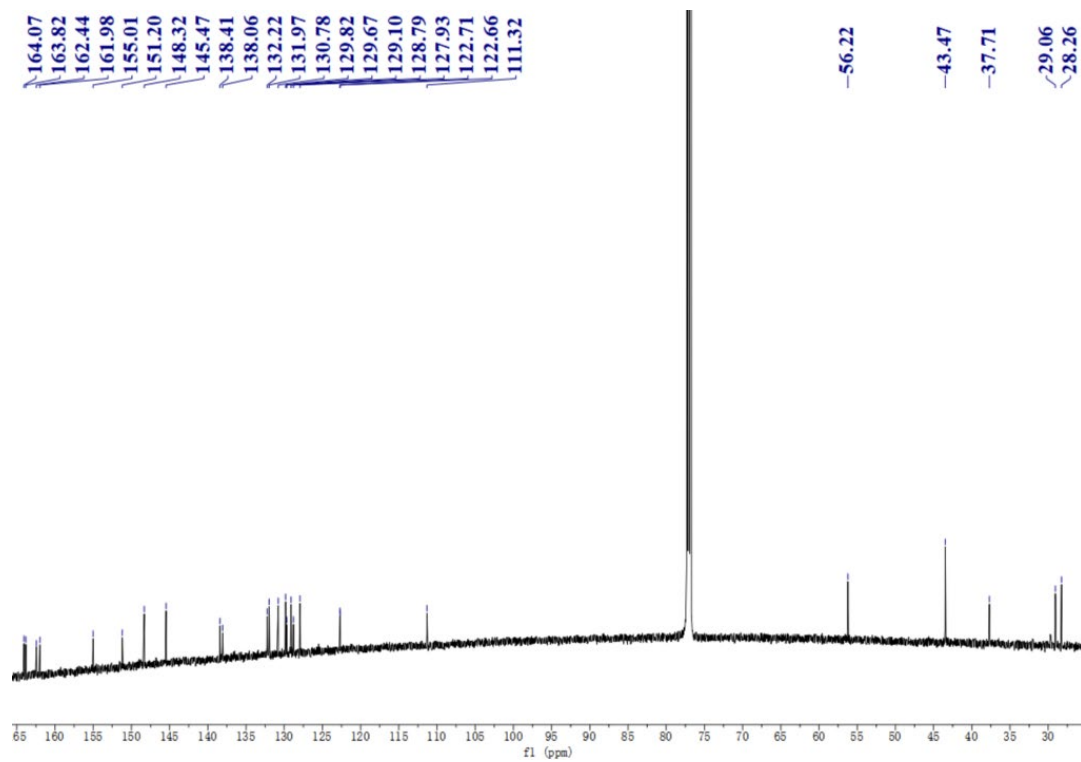
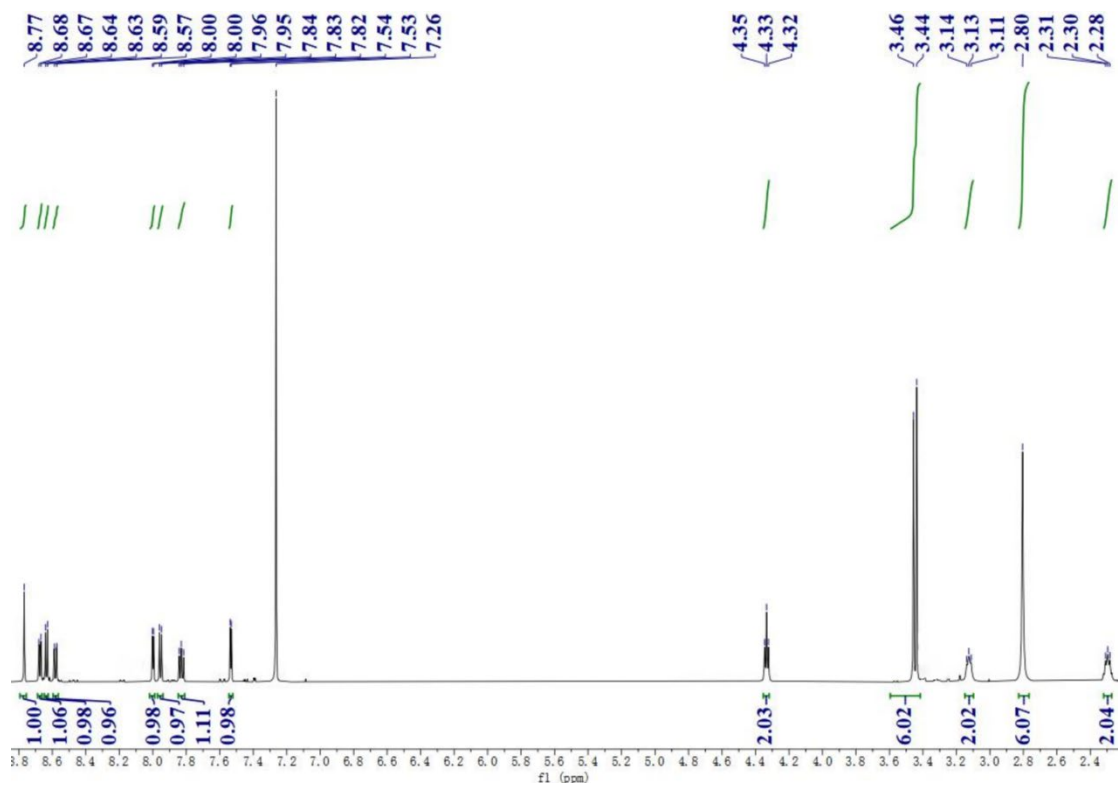


Fig. S8 ¹H NMR (top) and ¹³C NMR (bottom) spectra of NTTC.

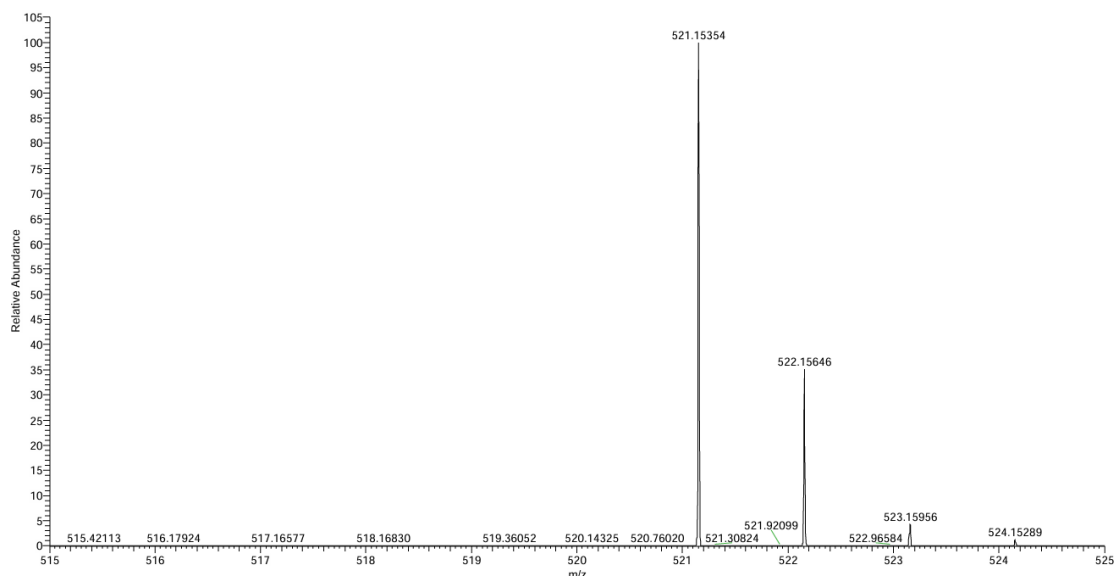


Fig. S9 ESI-MS Mass spectrum of NTDC.

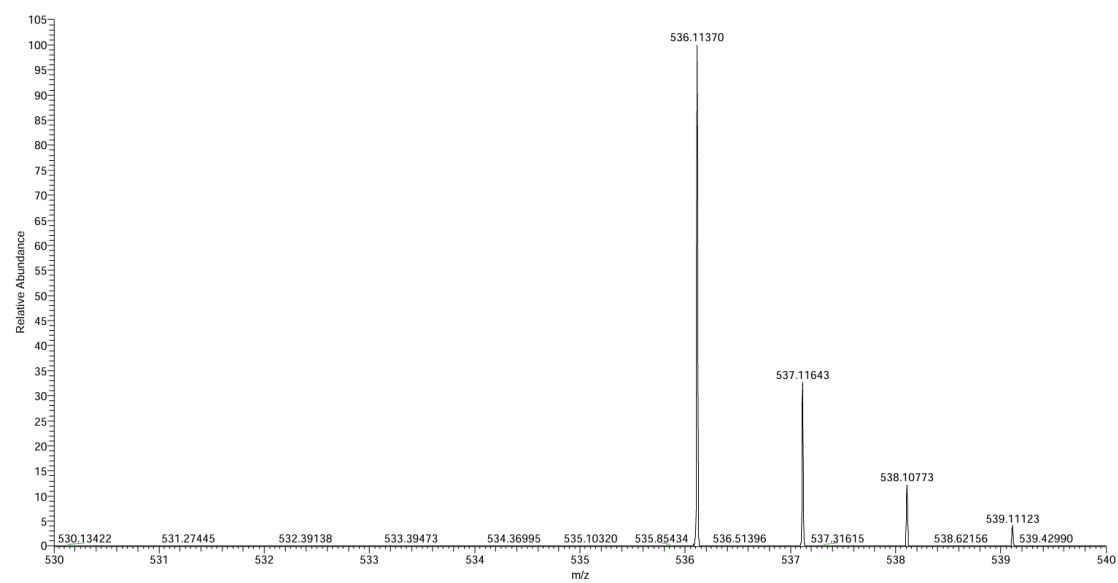


Fig. S10 ESI-MS Mass spectrum of NTR.

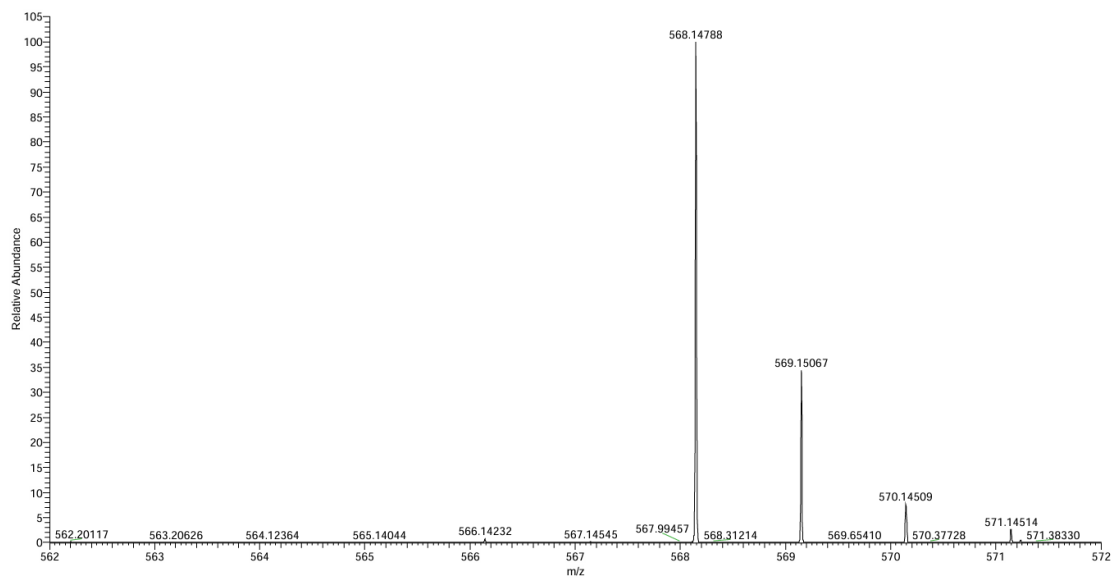


Fig. S11 ESI-MS Mass spectrum of NTRIC.

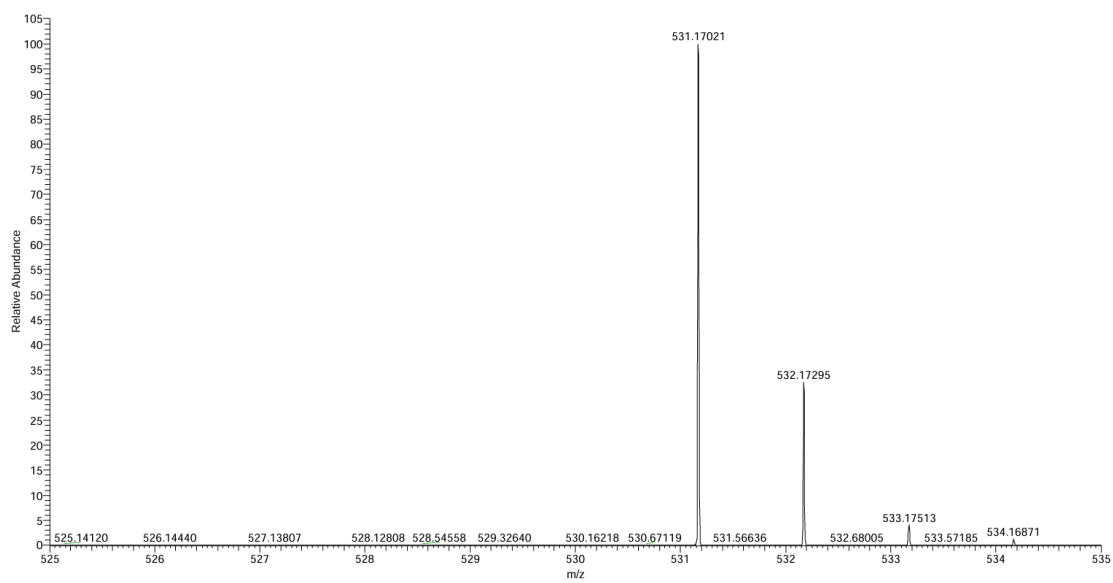


Fig. S12 ESI-MS Mass spectrum of NTTC.

Characterization

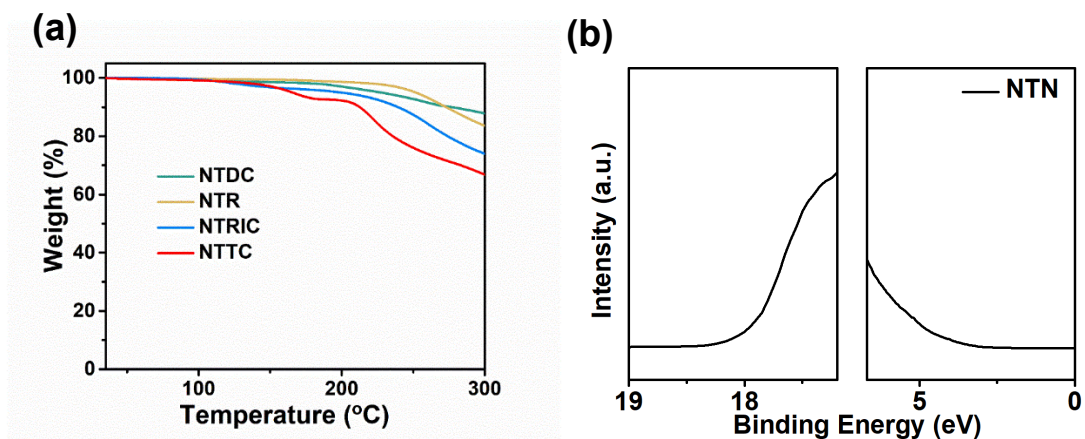


Fig. S13 (a) TGA spectra of NTDC, NTR, NTRIC, and NTTC, (b) UPS data of NTN.

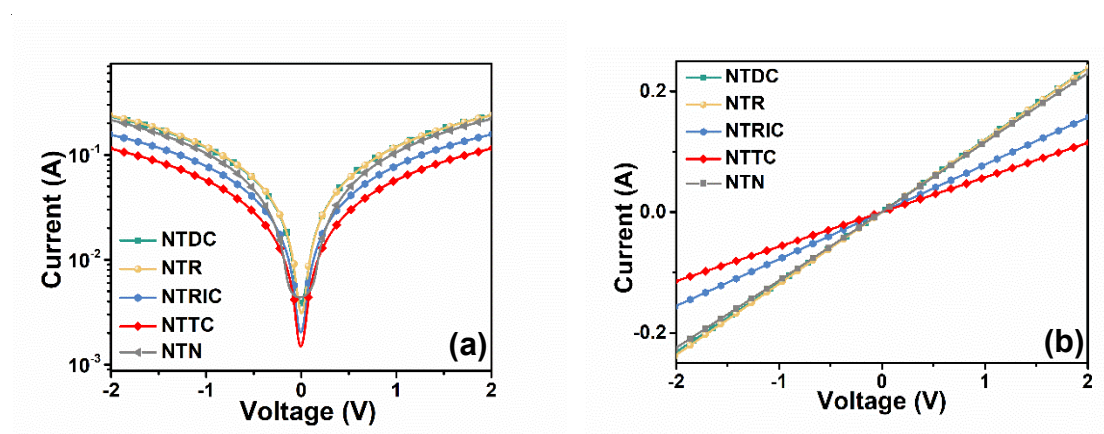


Fig. S14 (a) I - V tests of pure films on parallel Al electrode, and (b) I - V measurements data are plotted on linear-linear scale for NTDC, NTR, NTRIC, NTTC, and NTN, respectively.

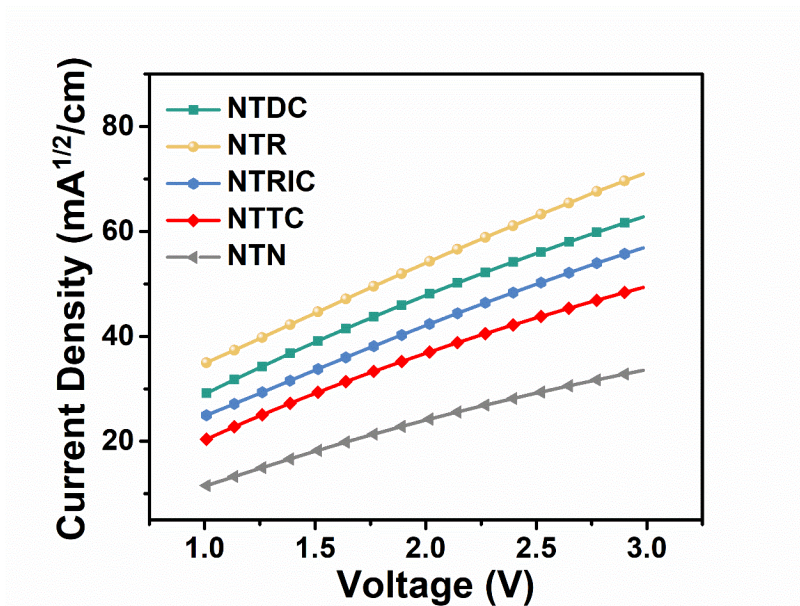


Fig. S15 J - V characteristics in the dark for electron-only devices based on NTDC, NTR, NTRIC, NTTC, and NTN, respectively.

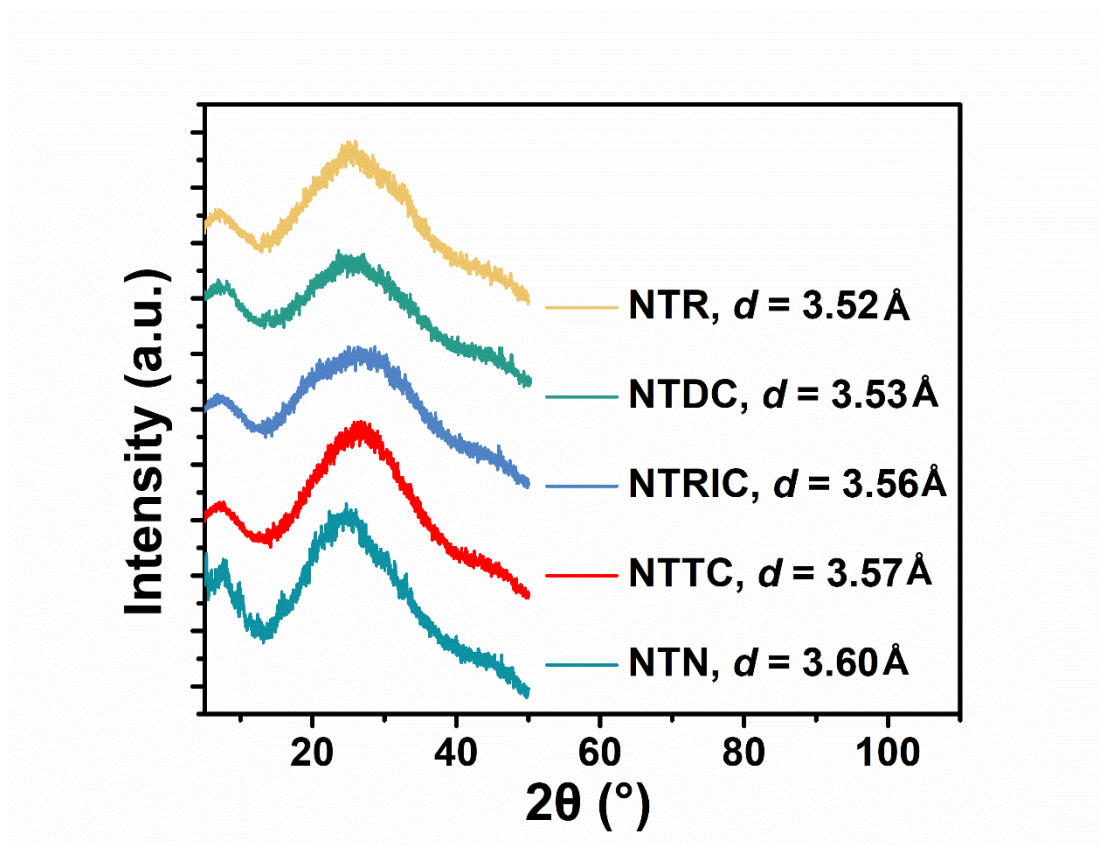


Fig. S16 XRD patterns and π - π stacking distances of NTR, NTDC, NTRIC, NTTC, and NTN.

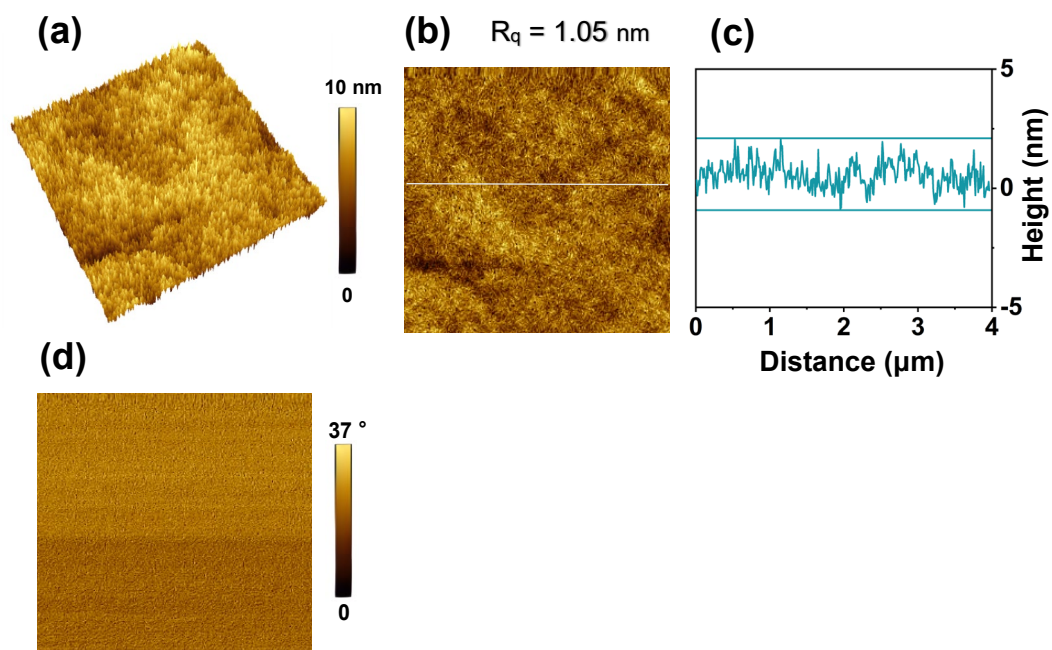


Fig. S17 AFM 3D image of roughness morphology (a), height image (b), roughness (c), and phase image (d) of NTN. The scale of image is $4.0 \mu\text{m} \times 4.0 \mu\text{m}$.

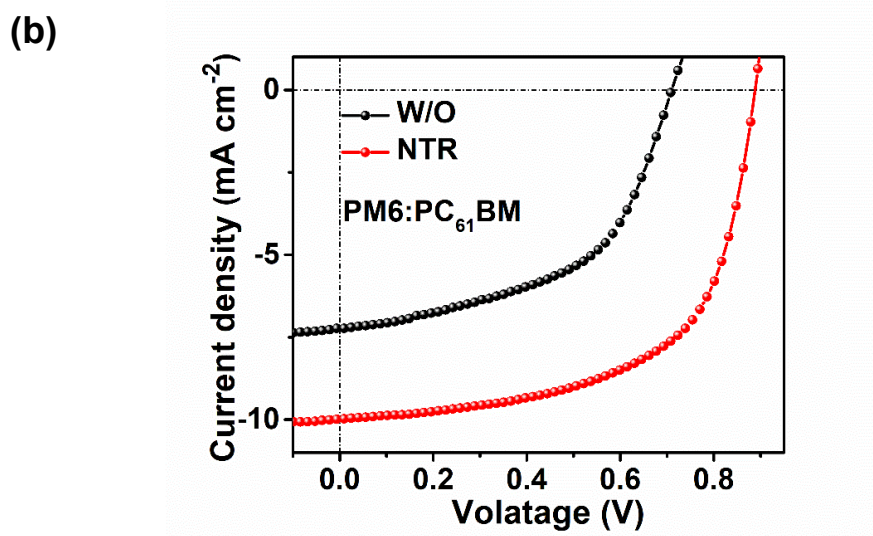
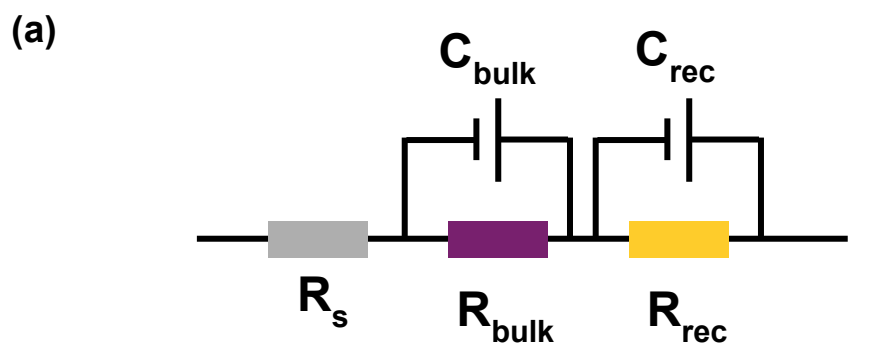


Fig. S18 Equivalent circuit diagram that be adopted for fitting the EIS spectroscopy (a), and photovoltaic performance of PM6:PC₆₁BM -based devices with or without NTR interlayer (b).

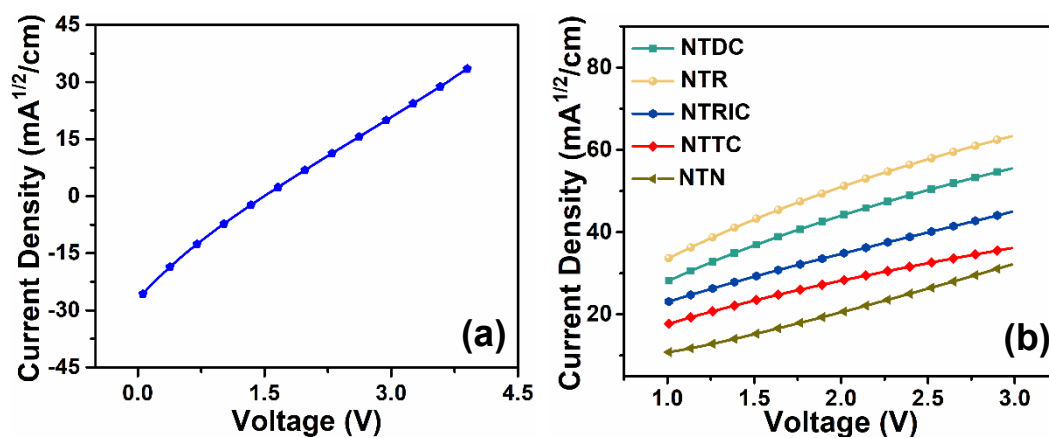


Fig. S19 J - V characteristics in the dark for hole-only device (a), and electron-only devices (b) based on NTDC, NTR, NTRIC, NTTC, and NTN, respectively.

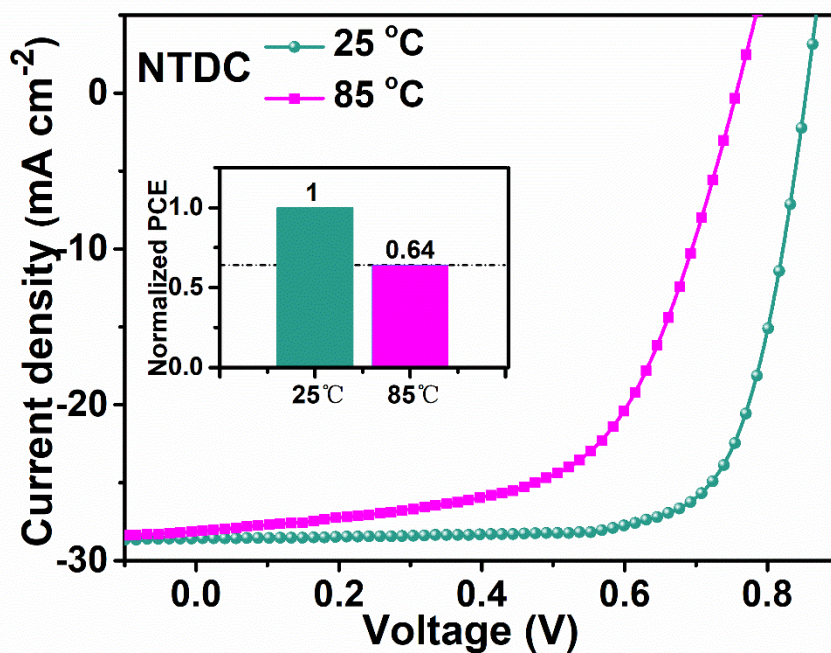


Fig. S20 Photovoltaic performances of the optimized fresh (25°C) and aged (85°C) PSCs with NTDC interlayer.

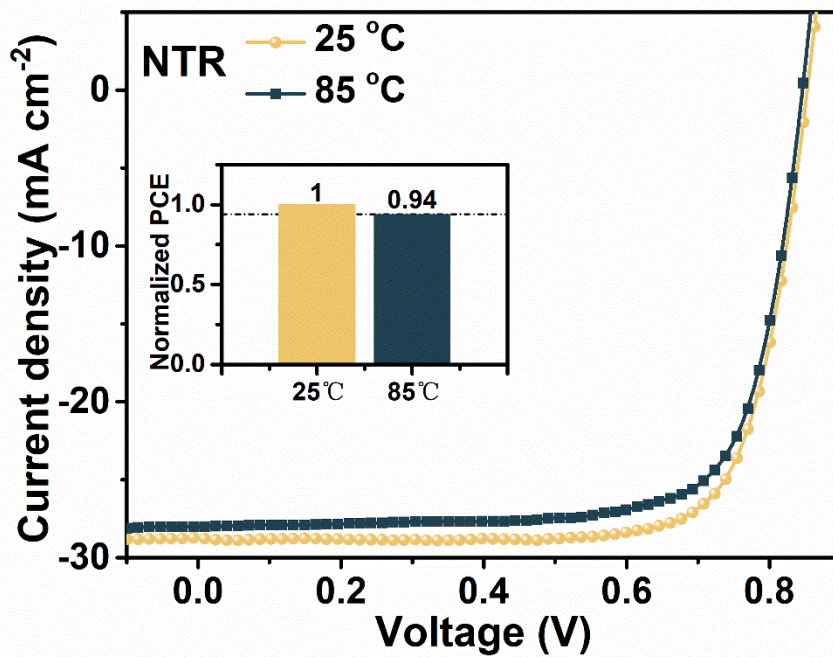


Fig. S21 Photovoltaic performances of the optimized fresh and aged PSCs with NTR interlayer.

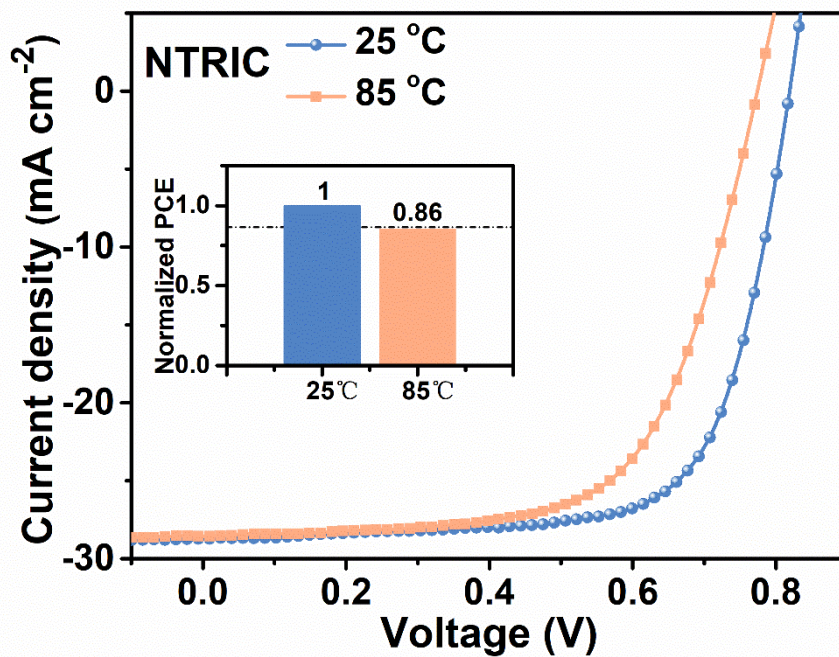


Fig. S22 Photovoltaic performances of the optimized fresh and aged PSCs with NTRIC interlayer.

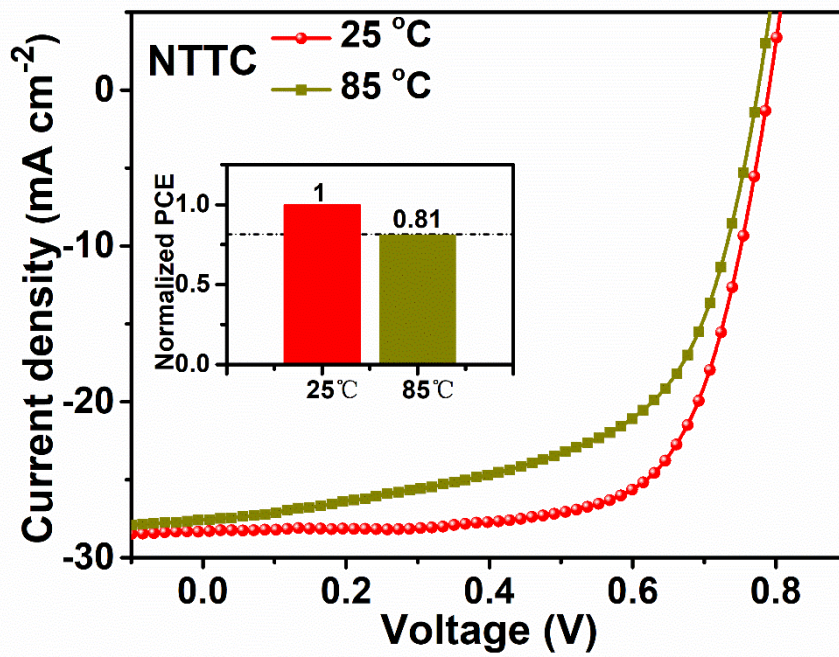


Fig. S23 Photovoltaic performances of the optimized fresh and aged PSCs with NTTC interlayer.

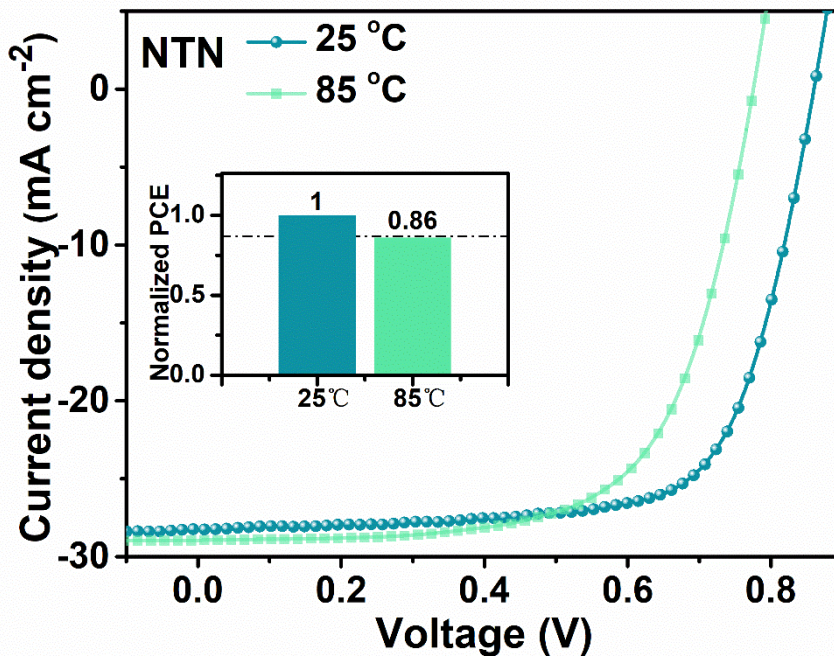


Fig. S24 Photovoltaic performances of the optimized fresh and aged PSCs with NTN interlayer.

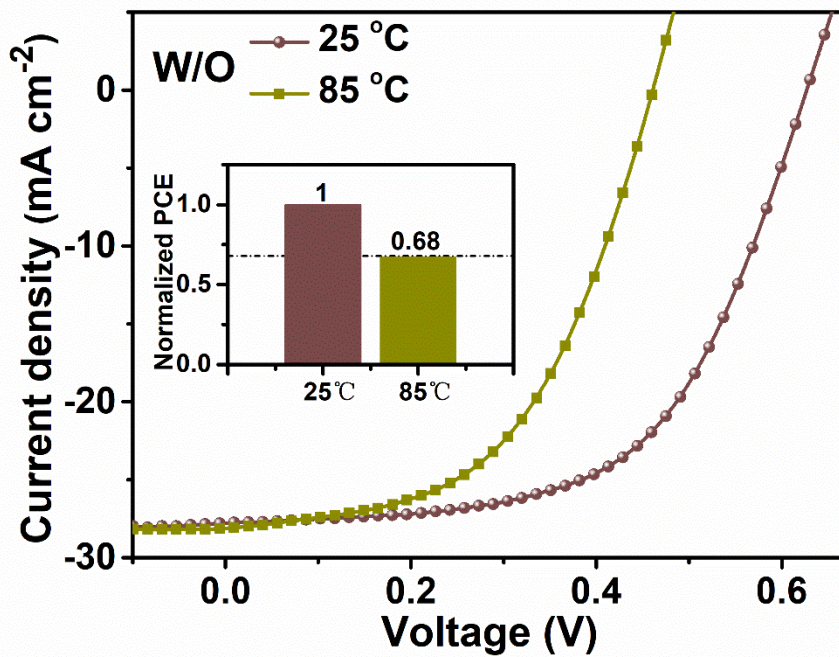


Fig. S25 Photovoltaic performances of the optimized fresh and aged PSCs without CIM.

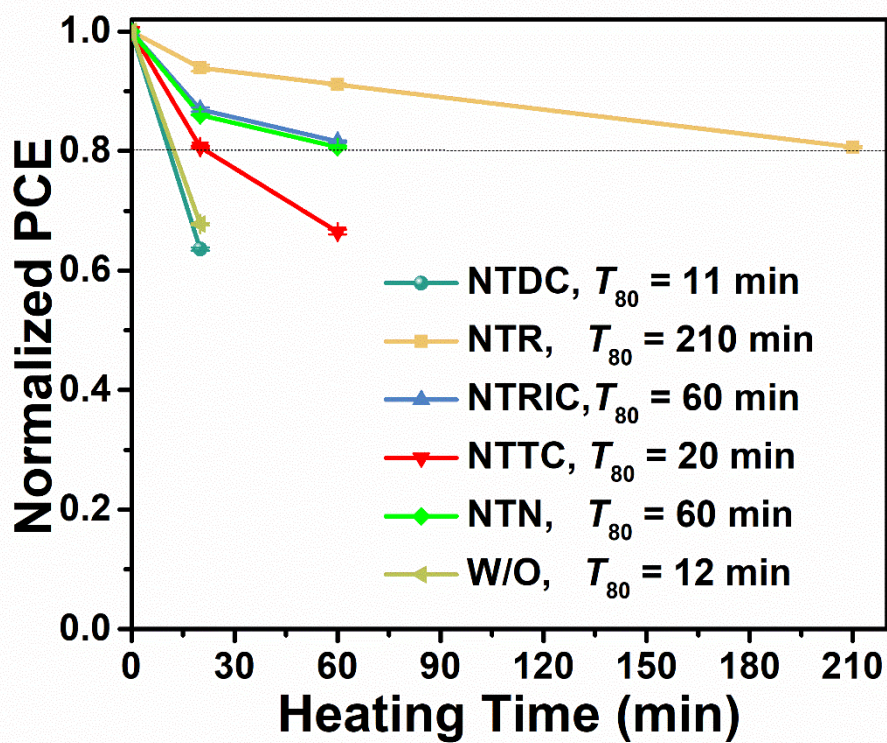


Fig. S26 T_{80} of the optimized aged PSCs at 85 °C.

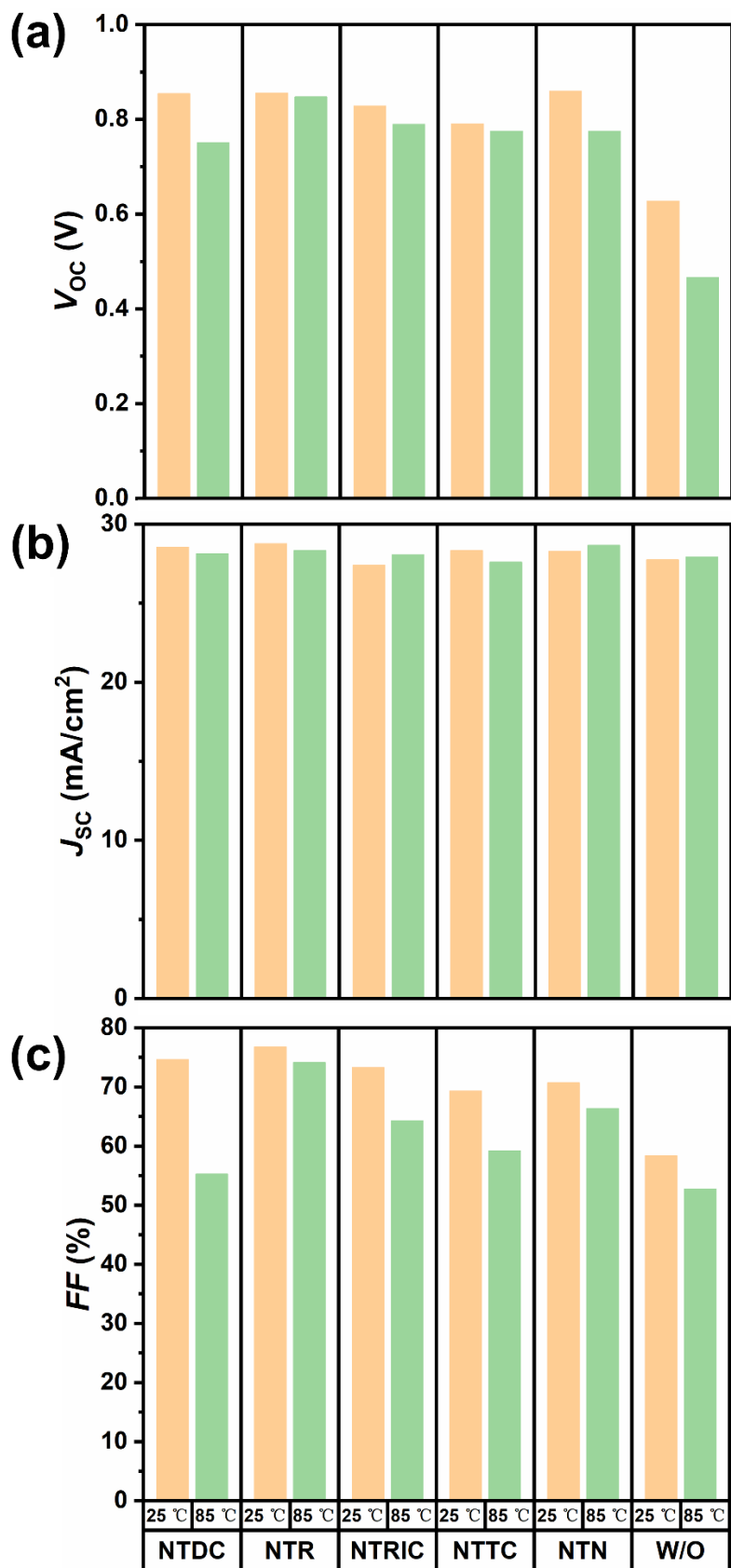


Fig. S27 The variations of V_{oc} (a), J_{sc} (b), and FF (c) parameters of the optimized fresh (orange) and aged (green) PSCs with or without CIMs.

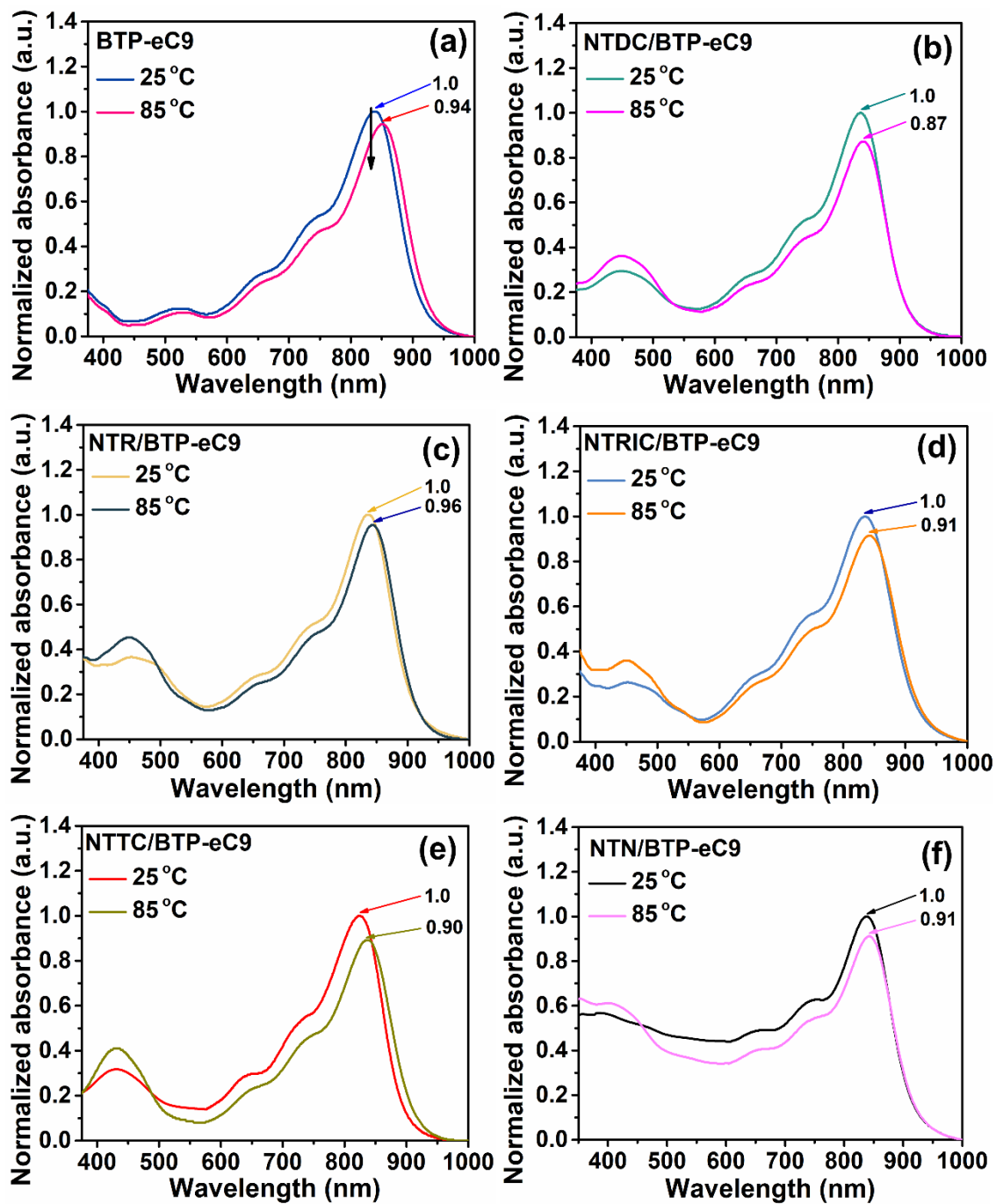


Fig. S28 UV-vis absorption spectra of the fresh (25 °C) and aged (85 °C) BTP-eC9 neat film and CIM/BTP-eC9 coated films.

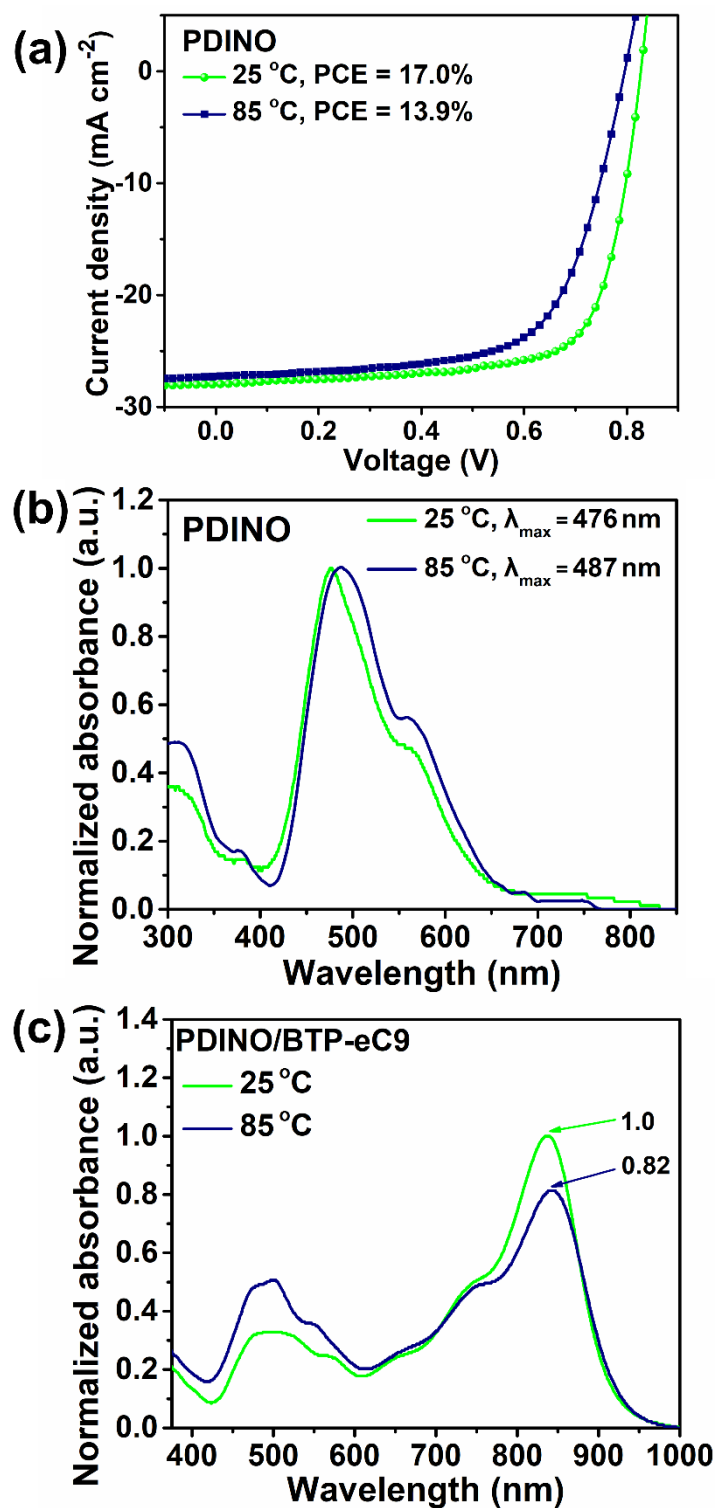


Fig. S29 Photovoltaic performances of the optimized fresh (25°C) and aged (85°C for 20 min) PSCs with PDINO interlayer.

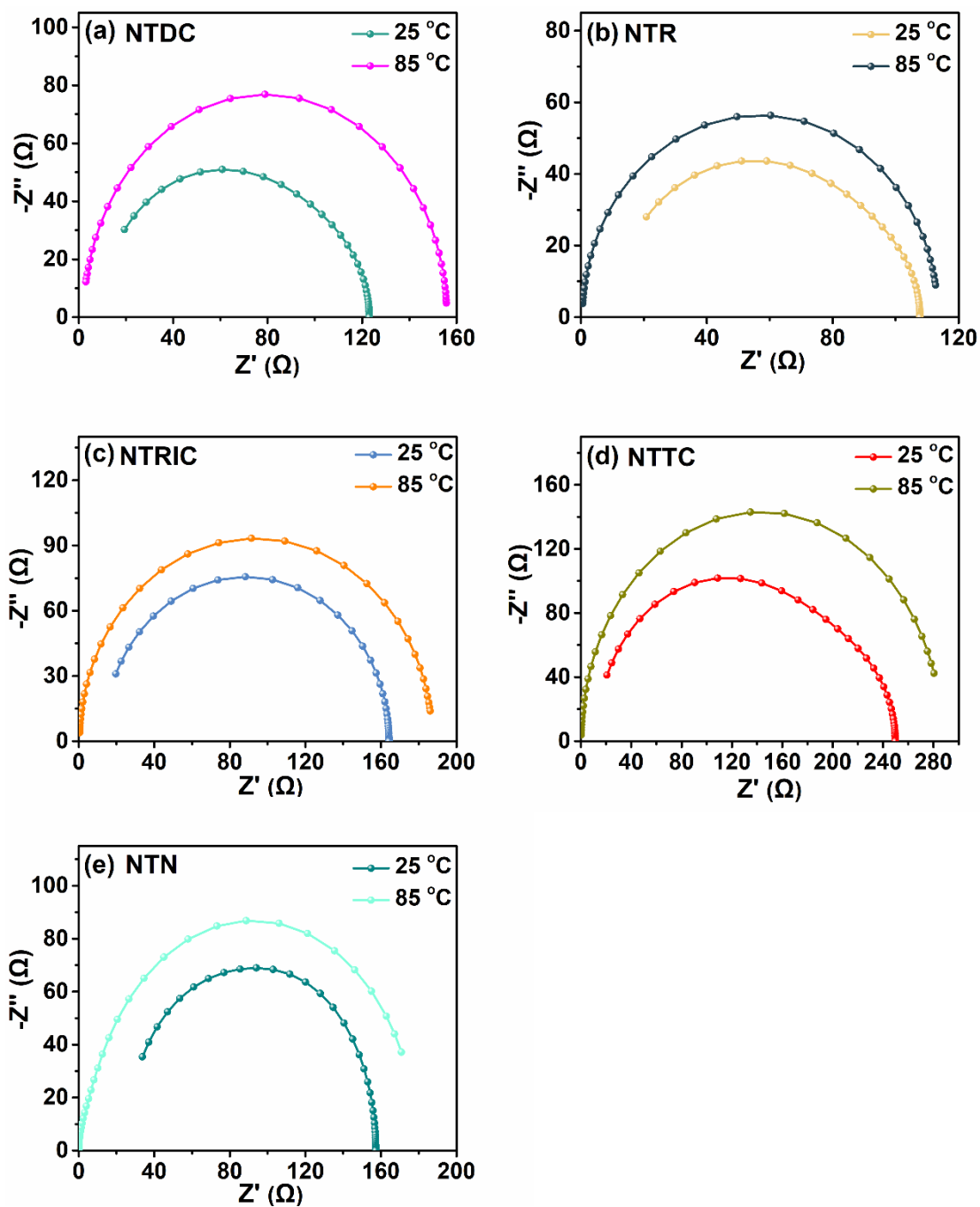


Fig. S30 Nyquist plots of the optimized fresh (25 °C) and aged (85 °C) devices based on NTDC, NTR, NTRIC, NTTC, and NTN interlayers.

Table S1 A summary of device performance of NI interlayers based binary PSCs

CIM	PAL	PCE (%) ^a	References	
NA	PM6:Y6	0.79	<i>ChemSusChem</i> , 2021, 14 , 4783–4792.	Our previous work
NAA		13.9		
NEA		15.0		
NT		1.3	<i>J. Colloid Interface Sci.</i> , 2022, 627 , 880–890.	
NTN		16.6		
N2TN		13.9		
NEN		1.2	<i>Chem. Eng. J.</i> , 2022, 441 , 135894.	
NTA		16.8		
ONTN		15.4	<i>Dyes Pigments</i> , 2023, 209 , 110911.	
ONBN		12.6		
NDT-1	PM6: BTP-eC9	13.2	<i>Chin. J. Struct. Chem.</i> , 2024, 43 , 100277.	
NDT-2		17.1		
3PNIN		17.7	<i>Nano Res.</i> , 2024, 17 , 1564–1570.	
3ONIN		16.8		
TT-N-N	PM6: Y6	17.48	<i>Angew. Chem., Int. Ed.</i> , 2024, DOI:10.1002/anie.202413135.	Work from another group
TT-N-M	PM6: BTP-eC9	18.44		
NTDC	PM6: BTP-eC9	18.2		This work
NTR		18.9		
NTRIC		17.1		
NTTC		15.6		

^aThe binary device structure: ITO/PEDOT:PSS/PAL/CIM/Al or Ag.

Table S2 The photovoltaic performance of PSCs based on NTR interlayer with different thickness

Thickness (nm)	V_{OC} (V)	J_{SC} (mA cm ⁻²)	FF (%)	PCE (%) ^a
7	0.849 (0.847 ± 0.002)	28.6 (28.4 ± 0.1)	75.5 (75.4 ± 0.1)	18.3 (18.1 ± 0.2)
10	0.855 (0.852 ± 0.003)	28.7 (28.6 ± 0.1)	76.9 (76.7 ± 0.2)	18.9 (18.7 ± 0.2)
15	0.846 (0.844 ± 0.003)	28.5 (28.3 ± 0.1)	75.5 (75.3 ± 0.2)	18.2 (18.0 ± 0.2)
21	0.833 (0.830 ± 0.003)	28.2 (28.0 ± 0.1)	75.8 (75.7 ± 0.1)	17.8 (17.6 ± 0.2)
27	0.829 (0.826 ± 0.003)	28.2 (28.1 ± 0.1)	72.4 (72.3 ± 0.1)	16.9 (16.8 ± 0.1)
32	0.825 (0.822 ± 0.003)	28.1 (28.0 ± 0.16)	71.7 (71.2 ± 0.5)	16.6 (16.4 ± 0.2)
36	0.829 (0.827 ± 0.002)	27.6 (27.5 ± 0.1)	71.6 (71.5 ± 0.1)	16.4 (16.3 ± 0.1)

^aAveraged values in parentheses from eight devices.**Table S3** The photovoltaic performance of PM6:PC61BM- based devices with or without NTR interlayer

NTR	V_{OC} (V)	J_{SC} (mA cm ⁻²)	FF (%)	PCE (%) ^a
N	0.710 (0.708 ± 0.002)	7.2 (7.0 ± 0.2)	52.9 (52.8 ± 0.1)	2.7 (2.6 ± 0.1)
Y	0.888 (0.885 ± 0.003)	9.9 (9.8 ± 0.1)	61.2 (61.0 ± 0.2)	5.4 (5.3 ± 0.1)

^aAveraged values in parentheses from five devices.

Table S4 Hole and electron mobilities of the optimized PSCs with NI interlayers

PSCs	μ_h ($10^{-4} \text{ cm}^2 \text{ V}^{-1} \text{ s}^{-1}$)	μ_e ($10^{-4} \text{ cm}^2 \text{ V}^{-1} \text{ s}^{-1}$)	μ_h/μ_e
NTDC-	5.0×10^{-4}	4.6	1.09
NTR-		5.4	0.93
NTRIC-		3.9	1.28
NTTC-		2.8	1.79
NTN-		4.0	1.25

Table S5 The photovoltaic performance of the optimized fresh (@25 °C) and aged (@85 °C for 20 min) PSCs

	V_{oc} (V)	J_{sc} (mA cm ⁻²)	FF (%)	PCE ^a (%)	PCE ratio ^b
NTDC -25 °C	0.854 (0.852 ± 0.002)	28.5 (28.3 ± 0.2)	74.4 (74.2 ± 0.02)	18.1 (17.9 ± 0.2)	0.64
NTDC -85 °C	0.750 (0.745 ± 0.005)	28.1 (28.0 ± 0.1)	55.2 (55.0 ± 0.2)	11.6 (11.5 ± 0.1)	
NTR -25 °C	0.855 (0.850 ± 0.005)	28.8 (28.5 ± 0.3)	76.4 (76.3 ± 0.1)	18.8 (18.5 ± 0.3)	0.94
NTR -85 °C	0.847 (0.843 ± 0.004)	28.3 (28.2 ± 0.1)	74.0 (73.9 ± 0.1)	17.7 (17.6 ± 0.1)	
NTRIC -25 °C	0.828 (0.826 ± 0.002)	27.4 (27.2 ± 0.2)	73.2 (73.1 ± 0.1)	16.6 (16.4 ± 0.2)	0.86
NTRIC -85 °C	0.789 (0.786 ± 0.003)	28.0 (27.9 ± 0.1)	64.2 (64.1 ± 0.1)	14.2 (14.1 ± 0.1)	
NTTC -25 °C	0.790 (0.786 ± 0.004)	28.3 (28.2 ± 0.1)	69.3 (68.9 ± 0.4)	15.5 (15.3 ± 0.2)	0.81
NTTC -85 °C	0.775 (0.766 ± 0.009)	27.6 (27.3 ± 0.3)	59.1 (58.9 ± 0.2)	12.6 (12.3 ± 0.3)	
NTN -25 °C	0.859 (0.857 ± 0.002)	28.2 (28.1 ± 0.1)	70.7 (70.6 ± 0.1)	17.1 (17.0 ± 0.1)	0.86
NTN -85 °C	0.775 (0.772 ± 0.003)	28.6 (28.5 ± 0.1)	66.3 (65.6 ± 0.7)	14.7 (14.4 ± 0.3)	
W/O -25 °C	0.627 (0.626 ± 0.002)	27.7 (27.6 ± 0.2)	58.3 (58.1 ± 0.2)	10.1 (10.0 ± 0.1)	0.68
W/O -85 °C	0.466 (0.465 ± 0.001)	27.9 (28.0 ± 0.1)	52.7 (52.6 ± 0.1)	6.9 (6.8 ± 0.1)	
PDINO -25 °C	0.832 (0.828 ± 0.004)	28.2 (28.1 ± 0.1)	72.5 (72.4 ± 0.1)	17.0 (16.8 ± 0.2)	0.82
PDINO -85 °C	0.770 (0.766 ± 0.004)	28.1 (28.0 ± 0.1)	64.4 (64.2 ± 0.2)	13.9 (13.8 ± 0.1)	

^aAveraged values in parentheses from eight devices.

^bPCE ratio = PCE_{@85°C} / PCE_{@25°C}.

Table S6 The photovoltaic performance of the aged PSCs heat-treated for 60 min^a

CIM	V_{oc} (V)	J_{sc} (mA cm ⁻²)	FF (%)	PCE ^b (%)
NTR	0.841 (0.838 ± 0.003)	28.1 (28.0 ± 0.1)	72.2 (72.0 ± 0.2)	17.1 (16.9 ± 0.2)
NTRIC	0.759 (0.757 ± 0.003)	27.8 (27.5 ± 0.3)	63.7 (63.1 ± 0.6)	13.4 (13.1 ± 0.3)
NTTC	0.692 (0.689 ± 0.003)	25.7 (25.5 ± 0.2)	57.5 (57.1 ± 0.4)	10.2 (10.0 ± 0.2)
NTN	0.764 (0.762 ± 0.002)	27.8 (27.5 ± 0.3)	63.6 (63.4 ± 0.2)	13.5 (13.3 ± 0.2)

^aHeating temperature is 85 °C. ^bAveraged values in parentheses from eight devices.

Table S7 The photovoltaic performance of the aged PSCs based on NTR interlayer with different heating time^a

heating time (min)	V_{oc} (V)	J_{sc} (mA cm ⁻²)	FF (%)	PCE ^b (%)
0	0.855 (0.850 ± 0.005)	28.8 (28.5 ± 0.3)	76.4 (76.3 ± 0.1)	18.8 (18.5 ± 0.3)
20	0.847 (0.843 ± 0.004)	28.3 (28.2 ± 0.1)	74.0 (73.9 ± 0.1)	17.7 (17.6 ± 0.1)
60	0.841 (0.838 ± 0.003)	28.1 (28.0 ± 0.1)	72.2 (72.0 ± 0.2)	17.1 (16.9 ± 0.2)
210	0.835 (0.832 ± 0.003)	26.9 (26.7 ± 0.2)	67.4 (67.2 ± 0.2)	15.1 (14.9 ± 0.2)

^aHeating temperature is 85 °C. ^bAveraged values in parentheses from eight devices.

Table S8 The d -spacing and d -spacing variation ($|\Delta d|$) of π - π stacking of CIM films

CIM	$d_{\text{fresh film}} (25\text{ }^{\circ}\text{C})$ (Å)	$d_{\text{aged film}} (85\text{ }^{\circ}\text{C})$ (Å)	$ \Delta d ^a$ (Å)
NTDC	3.53	3.70	0.17
NTR	3.52	3.50	0.02
NTRIC	3.56	3.46	0.10
NTTC	3.57	3.73	0.16
NTN	3.60	3.77	0.17

$$^a|\Delta d| = |d_{\text{fresh film}} - d_{\text{aged film}}|.$$

Table S9 The R_s of the optimized fresh (25°C) and aged (85°C) PSCs based on NI CIMs

CIM	$R_s (25\text{ }^{\circ}\text{C})$ (Ω)	$R_s (85\text{ }^{\circ}\text{C})$ (Ω)	ΔR_s^a (Ω)
NTDC	123.1	155.8	32.7
NTR	107.7	112.5	4.8
NTRIC	164.3	186.1	21.8
NTTC	249.8	280.5	30.7
NTN	157.3	170.9	13.6

$$^a\Delta R_s = R_{s, \text{aged PSC}} - R_{s, \text{fresh PSC}}.$$

References

- 1 P. Luo, K. An, L. Ying, G. Li, C. Zhu, B. Fan, F. Huang and Y. Cao, *J. Mater. Chem. C*, 2020, **8**, 5273–5279.
- 2 Q. Liao, Q. Kang, Y. Yang, C. An, B. Xu and J. Hou, *Adv. Mater.*, 2020, **32**, e1906557.
- 3 M. Zhang, X. Guo, W. Ma, H. Ade and J. Hou, *Adv. Mater.*, 2015, **27**, 4655–4660.
- 4 Y. Cui, H. Yao, J. Zhang, K. Xian, T. Zhang, L. Hong, Y. Wang, Y. Xu, K. Ma, C. An, C. He, Z. Wei, F. Gao and J. Hou, *Adv. Mater.*, 2020, **32**, e1908205.

5 P. N. Murgatroyd, *J. Phys. D Appl. Phys.*, 1970, **3**, 151–156.

6 Y. Zhao, Y. Liu, X. Liu, X. Kang, L. Yu, S. Dai and M. Sun, *ChemSusChem*, 2021, **14**,
4783–4792.